Paper presented at the European Two-Phase Flow Group Meeting,
Paris, May 29 - 31, 1989

Analysis of the Dryout Incident in the Oskarshamn 2 Boiling Water Reactor

K M Becker[1], J Engström[2], O Nylund[3],
B Schölin[3] and B Söderquist[1]

1) Royal Institute of Technology, S-100 44 STOCKHOLM
2) OKG AKTIEBOLAG, Box 1746, S-11187 STOCKHOLM
3) ABB Atom AB, S-721 63 VÄSTERÅS

Summary

Early in 1988 dryout of fuel rods occurred in the Oskarshamn 2 boiling water reactor. During re-fuelling it was observed that one corner rod was damaged in each of four fuel assemblies, which were of the SVEA design. The damaged zone covered about 180 degrees of the rod periphery facing the corner sub-channel, over a stretch of about 30 cm with the upper end just below the last downstream spacer.

The dominating cause of the dryout was re-use of fuel channels for ordinary 64-rod fuel, which were located in neighbouring positions to the SVEA fuel. The re-used fuel channels showed excessive bowing because of irradiation. This bow increased the water gap between the fuel assemblies, thus increasing the neutron moderation and the local power around one corner of the SVEA fuel. This and some other factors caused the local peaking factor for the corner rod to increase from ~1.04 to ~1.38.

The flow and power conditions in the damaged fuel assemblies were calculated by means of the POLCA, PHOENIX, CASMO and CONDOR computer programs. The results of these calculations were used as base for dryout predictions, which were carried out employing eight correlations, which are available in the open literature. The Barnett, the Becker and the Bezrukow correlations predicted the dryout power within 1 percent. Also the Condie-Bengston, the EPRI and the XN-1 correlations yielded very good results with accuracies of respectively 5.2, 7.9 and -7.2 percent. The Becker, the XN-1, the Bezrukow and the Condie-Bengston correlations predicted dryout to occur inside of the observed dryout zone of 30 cm length.

It is concluded that the dryout in the Oskarshamn 2 nuclear power plant was not causd by any faults in the design or manufacture of the SVEA fuel, and that the re-use of fuel channels should not be permitted.

List of Contents

1. INTRODUCTION

During the refuelling outage in August 1988 of the Oskarshamn 2 reactor, four failed fuel assemblies were identified through sipping. In the preceding cycle, offgas and primary system water activity had shown fuel leakage to develop stepwise in the period from January to February. From inspections it was subsequently concluded that dryout had caused the fuel rod failure through heavy cladding oxidation of one single rod at the control rod corner in each of the four assemblies. The dryout region was located immediately below the topmost spacer grid and water intrusion had given rise to secondary cladding failures near the bottom end. Dryout had occurred over a stretch of about 30 cm. The damaged zone did not cover the total periphery of the rod, but rather about 180 degrees facing the corner sub-channel of the bundle.

All types of events that could have caused dryout, such as full power normal operation, nuclear heating at low system pressure, a power ascension at end-December, possible transients and operator errors were investigated. It was concluded that dryout occurred at full, steady state power since reanalysis of the operation explains the failures, and other possibilities could be ruled out.

This dryout incident offers, indeed, an interesting possibility to carry out assessments of computer codes and dryout correlations as well as post-dryout heat transfer correlations. In the present report predictions of the Oskarshamn 2 in-pile dryout conditions are presented, employing a number of the mostly used rod bundle dryout correlations, which are available in the open literature.

2. TYPE OF FUEL AND CAUSE OF FUEL ROD OVERPOWER

The damaged fuel was of the SVEA-64 type, which is characterized by a water cross dividing the assembly into four channels, each containing a 4x4 rod bundle, as shown in Figure 1. The water cross improves the neutron moderation and thus increases reactivity and decreases local power and burnup peaking factors. It also improves the mechanical structure of the channel, so that lattice improvements can be made by decreasing the control rod gaps.

Power peaking factors should be modelled correctly for the mixed gap situation throughout the transition period. However, this was not done in the present case.

These two effects, as illustrated in Figure 3, resulted in much enlarged water gaps and a corresponding local improvement of the neutron moderation and power increase in the fuel rods facing these gaps. Especially the power in the corner rods of the SVEA bundles became very high. Figure 4 shows the rod power distribution used in the core supervision and as recalculated with the enlarged gaps according to Figure 3 C. The 8x8 channel bow was chosen to 4.5 mm, which is about 60% of the measured mid-channel bow. The justification for the use of this value for the presented dryout assessments is discussed later. Based on manufacturing data the SVEA assemblies had a mean bow of ~0.5 mm away from the control rod. The recalculated power distribution is seen to be strongly tilted and an average rod peaking factor of 1.38, normalized to 63 active rods, is found for the corner rod facing the centre of the supercell. This high local power, which was unknown to the reactor operating personnel, caused the dryout to occur on the corner rod.

It should also be noted that all the SVEA assemblies in the supercells in which the failures occurred were operating in their first cycle. This means that they were in a phase of increasing power as their content of burnable absorber was being depleted. The high local power also caused a high depletion rate of the burnable absorber in this region. Dryout therefore occurred earlier in the cycle than the predicted minimum dryout margin according to the core supervision calculations.

3. CONDITIONS IN THE FUEL ASSEMBLIES AT DRYOUT

Visual observation of the failed fuel assemblies after removal from the reactor showed, for one corner rod in each assembly, a distinct dryout area covering an axial stretch starting at about $z = 310$ cm and ending at $z = 339$ cm from the inlet. The end of the dryout zone was just below the upper spacer. The length of the heated section was 371.2 cm. The excessive heating covered approximately 180 degrees of the circumference of the rod; 90 degrees facing the corner sub-channel and about 45 degrees facing each of two neighbouring sub-channels as shown in the figure below

Outer supercells:

$$Q = 6.20 \text{ MW}$$
$$\dot{m} = 9.50 \text{ kg/s}$$

The central supercell was chosen for the present assessment because the channel bow situation is best known in this case.

The rod power distribution of a SVEA assembly in the central supercell, with mean channel deflections according to Figure 3 C, has already been shown in Figure 4. It was calculated with the PHOENIX program. The assumption of an axial mean deflection of about 60% of the measured mid-channel values for the 8x8 channels accounts for the axial variation of the channel deflection, and further for the possibility that the maximum deflection could have been somewhat smaller when the dryout occurred. The axial power distribution, obtained by POLCA, is shown in Figure 7.

The large difference between the powers in the four quadrants of the fuel has a significant influence on the mass flow rate through the quadrants. The CONDOR program was used to calculate the flows, and for the quadrant where dryout occurred the following result was obtained:

Mass flow rate $\dot{m} = 2.13$ kg/s

Reverting to Figure 4, the power and the local peaking factor for this quadrant became:

$$Q = 1.766 \text{ MW}$$
$$F_i = 1.152$$

Thus, the dryout predictions carried out in the following paragraphs, were based on the following parameters:

In the present study the local as well as the total power hypothesis were employed.

The total power hypothesis assumes the axial power distribution to be uniform. The dryout power is then easily calculated, but no information about the axial dryout position is obtained.

The employment of the local power hypothesis, however, yields the dryout power as well as the axial dryout position. Figure 8 shows the principle of the local hypothesis in a plot of the heat flux, q", versus the steam quality, x. For the bundle operating conditions the heat flux is plotted versus the steam quality along the bundle. The dotted line refers to the average heat flux and the solid line refers to the highest loaded rod. The steam quality is the average value over the cross-section, neglecting steam quality and mass velocity variations between the sub-channels of the fuel element.

For given pressure, inlet water temperature, mass velocity and geometry any dryout correlation can be reproduced in a heat flux versus steam quality plot as shown in the figure. The heat balance equation for an arbitrary axial position can be written

$$x = \frac{Q_T \int_0^{z/L} F_A\,(z/L)\,d(z/L)}{GFr} \cdot \frac{\Delta i_s}{r}$$

The equation reveals the existence of a linear relationship between the steam quality, x, and the fuel element power, Q, for all axial positions, z. A family of straight lines, representing an arbitrarily chosen number of axial positions can be drawn. The crossing points between the straight lines and the correlation yields a family of dryout heat fluxes and a family of dryout margins

$$\eta_{DOz} = \frac{q''_{DOz}}{q''_z}$$

The axial position, z, which gives the minimum value of η_{DO}, is the axial dryout position z_{DO}, and the corresponding intersection between the heat

As previously mentioned, the total power hypothesis does not give any information about the axial location of the dryout. In the next paragraph, were the local hypothesis is employed, predictions of the dryout power as well as the axial dryout location will be presented.

6.2 Local Hypothesis

The predictions with the local hypothesis are shown in Figures 9 to 16 and in Table 1. A comparison between the predictions is given in Figure 17. A summary of the predicted dryout powers and dryout locations is given in the table below.

Correlation	Q_{DO} MW	z_{DO} cm	Error
Barnett	1.78	353.1	0.6
Becker	1.77	324.8	0.0
Bezrukow	1.75	309.3	1.1
Biasi	2.55	324.8	-30.6
Condi-Bengston	1.68	309.3	5.2
CISE 4	2.12	340.3	-16.6
EPRI	1.64	371.2	7.9
XN-1	1.90	324.8	-7.2

In the Oskarshamn 2 sub-bundle the power was 1.77 MW, and dryout occurred on the corner pin facing the corner sub-channel on a stretch starting at z ~ 310 cm and ending at z = 339 cm. Neglecting the effect of the spacers one may then assume the middle value of z = 324 cm, to be a best estimate of the dryout position. Experience from loop experiments and evidence from the hot cell investigations, however, points to the upper end of the region, just below the topmost spacer, as the actual starting point of the dryout.

With regard to the dryout power excellent predictions within 1% were obtained with the Barnett, the Becker and the Bezrukow correlations.Also the Condie-Bengston, the EPRI and the XN-1 correlations yield very good results. However, the EPRI and the Barnett corrrelations do not predict

progress to improve the knowledge of the actual conditions as far as possible.

The actual power for onset of dryout has been somewhat exceeded during the incident. The fact that the damage was obtained only in the zone below the topmost spacer indicates that the limit was only marginally exceeded. Experience from loop tests suggests that damage would otherwise also have been obtained just below the next spacer in the upstream direction at z ~280 cm. Reverting to Figure 4 one observes that two of the rods, which are neighbours to the corner rod, had local peaking factors of 1.36, while the value for the corner rod was 1.38. This difference, which is less than 1.5 % suggests that also these rods should have been close to dryout. However, none of them were damaged.

It is therefore concluded that the dryout conditions for the corner rods are accuretely defined. With the reservation for some remaining uncertainties in the initial analysis the Oskarsham 2 incident therefore represents a very good base for assessments of dryout correlations.

6.3 Correlation Used in Core Supervision

The core supervision of the SVEA assemblies in Oskarshamn 2 relies on the commercial AA-74S correlation, which is based on extensive full scale testing. It includes a simplified sub-channel model that accounts for the local power distribution within the sub-bundles, and a routine that handles the power and flow mis-match between the sub-bundles. For the present case it gave a dryout power, which was high by 7 percent. Considering the uncertainties involved in this comparison of a quite extreme situation, as discussed above, that discrepancy may not be too surprising. However, because of the importance for the core supervision there is a continued effort to identify possible errors in all steps involved, and thus to be able to further improve the overall accuracy of the in-core dryout evaluation.

8. CONCLUSIONS

On the basis of the present work the following conclusions were obtained:

1. Several rod bundle dryout correlations, which are available in the open literature, predict accurately the dryout conditions for the Oskarshamn 2 dryout incident.

2. The effects of irradiation on channel bow should be recognized as a serious core supervision problem, and the re-use of channels should therefore be avoided.

3. The effect of channel bow should be incorporated in the calculations of the power distributions in the fuel assemblies. If this is considered it is not necessary to change the dryout margin.

4. The dryout in the Oskarshamn 2 reactor was not caused by any faults in the design or manufacture of the fuel.

8. Bezrukow Y A et. al
Experimental Investigation and Statistical Analysis of Data on Burnout in Rod Bundles for Water-Moderated Water-Cooled Reactors. Teploenergetika, Vol 23, 67-70 (1976)

9. Biasi L et. al
Studies on Burnout, Part 3. A new Correlation for Round Ducts and Uniform Heating and its Comparison with World Data. Energia Nucleare, Vol 12. No 9, 1967

10. Condie K G and Bengston S J
Development of the MOD7 CHF Correlation. PN-181-76, E.G & G. Idaho, 1978

11. Gaspari G P et. al
A rod Centered Subchannel Analysis with Turbulent Mixing for Critical Heat Flux Predictions in Rod Clusters Cooled by Boiling Water. Proc, of the 5th International Heat Transfer Conference, Tokyo, September 1974

12. Reddy D G and Fighetty C F
Parametric Study of CHF Data. Vol 2, 1983 (EPRI NP-2609)

13. Steves L H et. al
XN-1 Critical Heat Flux Correlation for Boiling Water Reactor Fuel. 1972 (JN-72-18)

14. Lee D H and Obertelli J D
An Experimental Investigation of Forced Convection Burnout in High Pressure Water - II Preliminary Results for Round Tubes with Non-Uniform Axial Heat Flux Distribution. 1963 (AEEW-R309)

15. Bertoletti S et. al
Heat Transfer Crisis with Steam-Water Mixtures. Energia Nucleare 12, 1965

Table 1

EXPERIMENTAL AND PREDICTED BURNOUT CONDITIONS
EXPERIMENTS: O2 SVEA-64
CORRELATION: BARNETT, LOCAL HYPOTHESIS

L cm	D cm	N	P0 cm	PH cm	F cm2	F(1)
371.2	1.225	16	25.6	61.6	24.3	1.152

RUN	P bar	DELTAH kJ/kg	G kg/m2,s	QTEXP MW	QAEXP W/cm2	XEXP	QTPRE MW	QAPRE W/cm2	XPRE	ZBO cm	ERROR %
1	70.5	60.3	877.3	1.77	56.2	0.508	1.78	56.6	0.511	353.1	-.6

EXPERIMENTAL AND PREDICTED BURNOUT CONDITIONS
EXPERIMENTS: O2 SVEA-64
CORRELATION: BECKER, LOCAL HYPOTHESIS

L cm	D cm	N	P0 cm	PH cm	F cm2	F(1)
371.2	1.225	16	25.6	61.6	24.3	1.152

RUN	P bar	DELTAH kJ/kg	G kg/m2,s	QTEXP MW	QAEXP W/cm2	XEXP	QTPRE MW	QAPRE W/cm2	XPRE	ZBO cm	ERROR %
1	70.5	60.3	877.3	1.77	76.2	0.476	1.77	76.2	0.476	329.8	0.0

EXPERIMENTAL AND PREDICTED BURNOUT CONDITIONS
EXPERIMENTS: O2 SVEA-64
CORRELATION: DEZRUKOV, LOCAL HYPOTHESIS

L cm	D cm	N	P0 cm	PH cm	F cm2	F(1)
371.2	1.225	16	25.6	61.6	24.3	1.152

RUN	P bar	DELTAH kJ/kg	G kg/m2,s	QTEXP MW	QAEXP W/cm2	XEXP	QTPRE MW	QAPRE W/cm2	XPRE	ZBO cm	ERROR %
1	70.5	60.3	877.3	1.77	81.5	0.455	1.73	80.7	0.450	309.3	1.1

EXPERIMENTAL AND PREDICTED BURNOUT CONDITIONS
EXPERIMENTS: O2 SVEA-64
CORRELATION: BIASI, LOCAL HYPOTHESIS

L cm	D cm	N	P0 cm	PH cm	F cm2	F(1)
371.2	1.225	16	25.6	61.6	24.3	1.152

RUN	P bar	DELTAH kJ/kg	G kg/m2,s	QTEXP MW	QAEXP W/cm2	XEXP	QTPRE MW	QAPRE W/cm2	XPRE	ZBO cm	ERROR %
1	70.5	60.3	877.3	1.77	76.2	0.476	2.35	109.8	0.703	324.8	-30.6

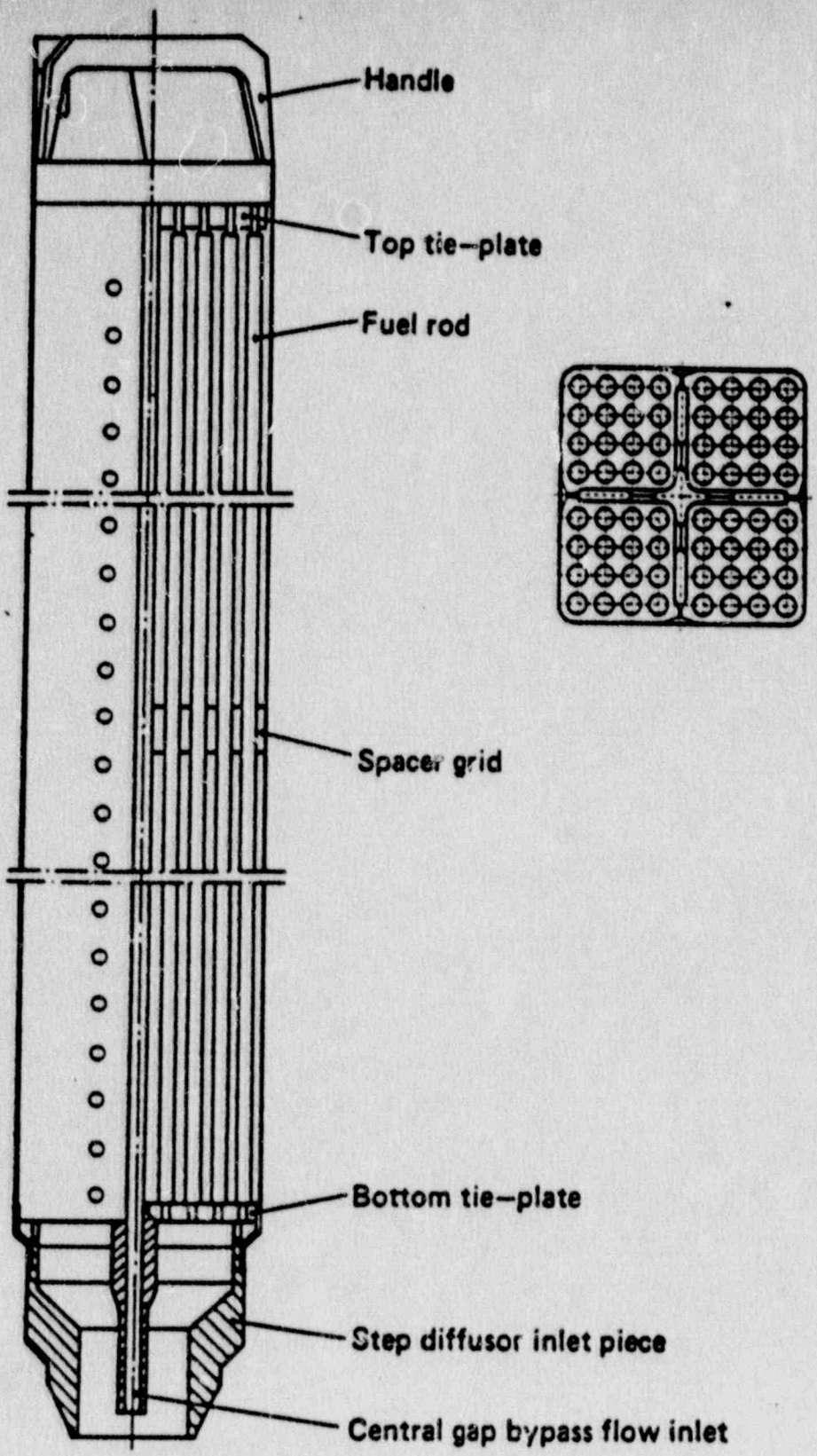

Figure 1. SVEA fuel assembly

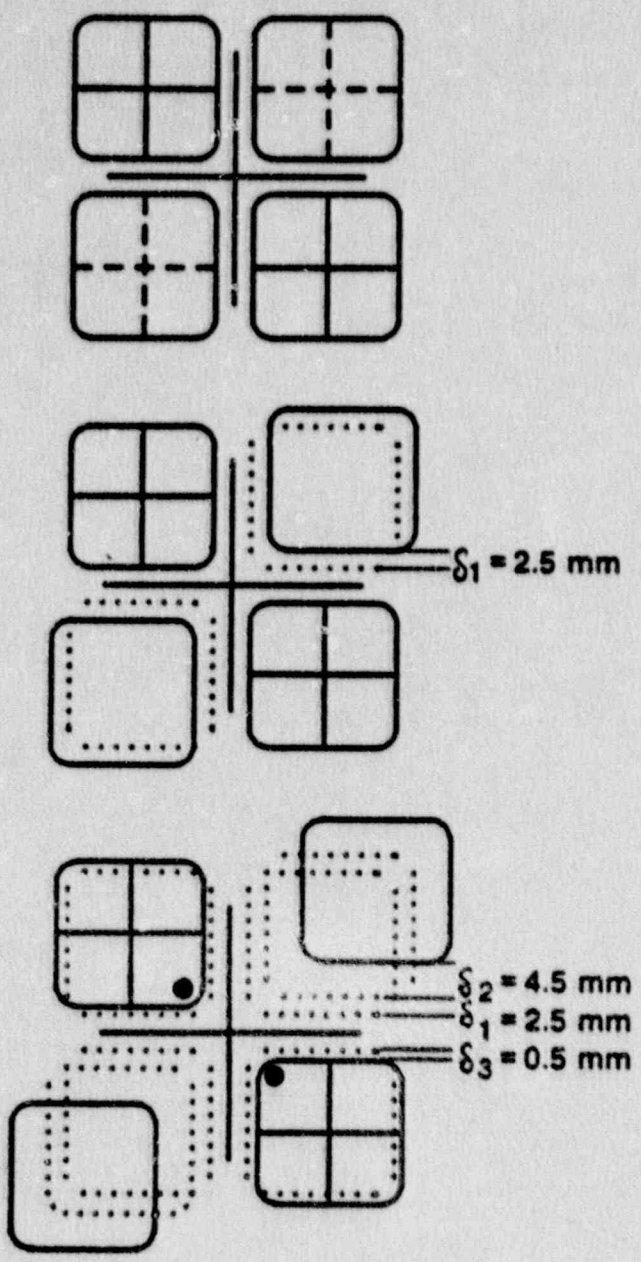

A. Nominal gaps of full SVEA core assumed in plant core supervision

B. Nominal gaps in mixed core

C. Assumed axial mean gaps with channel bow at dryout failure, based on measured 8 × 8 mid-channel bow values of 7-8 mm at the end of cycle

Figure 3. Water gap changes in Oskarshamn 2 core cell

Front view Side view

The pictures have been put together by a number of smaller photos.

Cladding is seen to be strongly oxidized. Layers of oxide have been peeled off in high temperature zone.

Cladding creep down has occurred at the pellet boundaries as a result of over-temperature and external overpressure.

Figure 6. Hot cell pictures of lower end of dryout zone

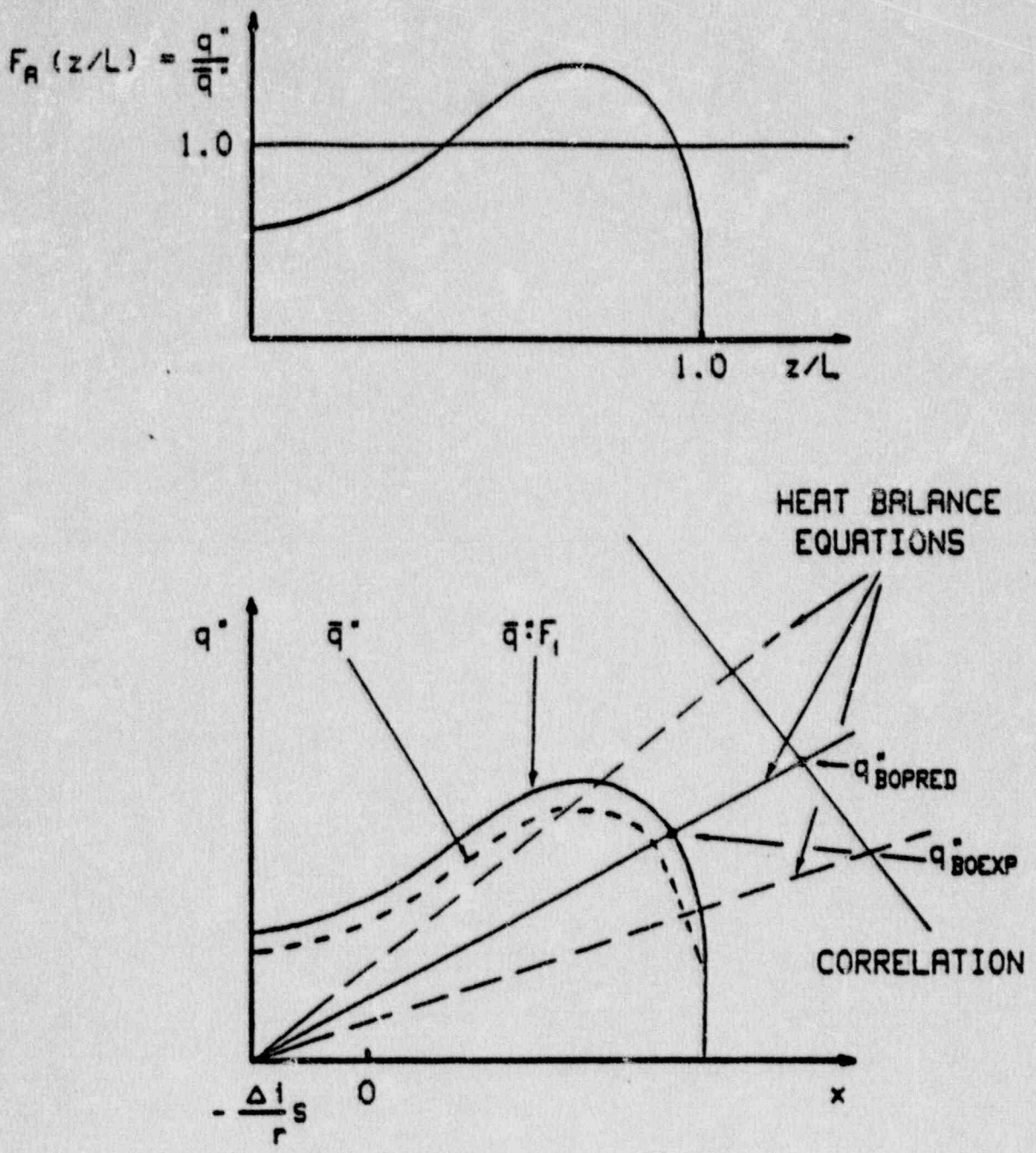

Figure 8. Principle of local hypothesis

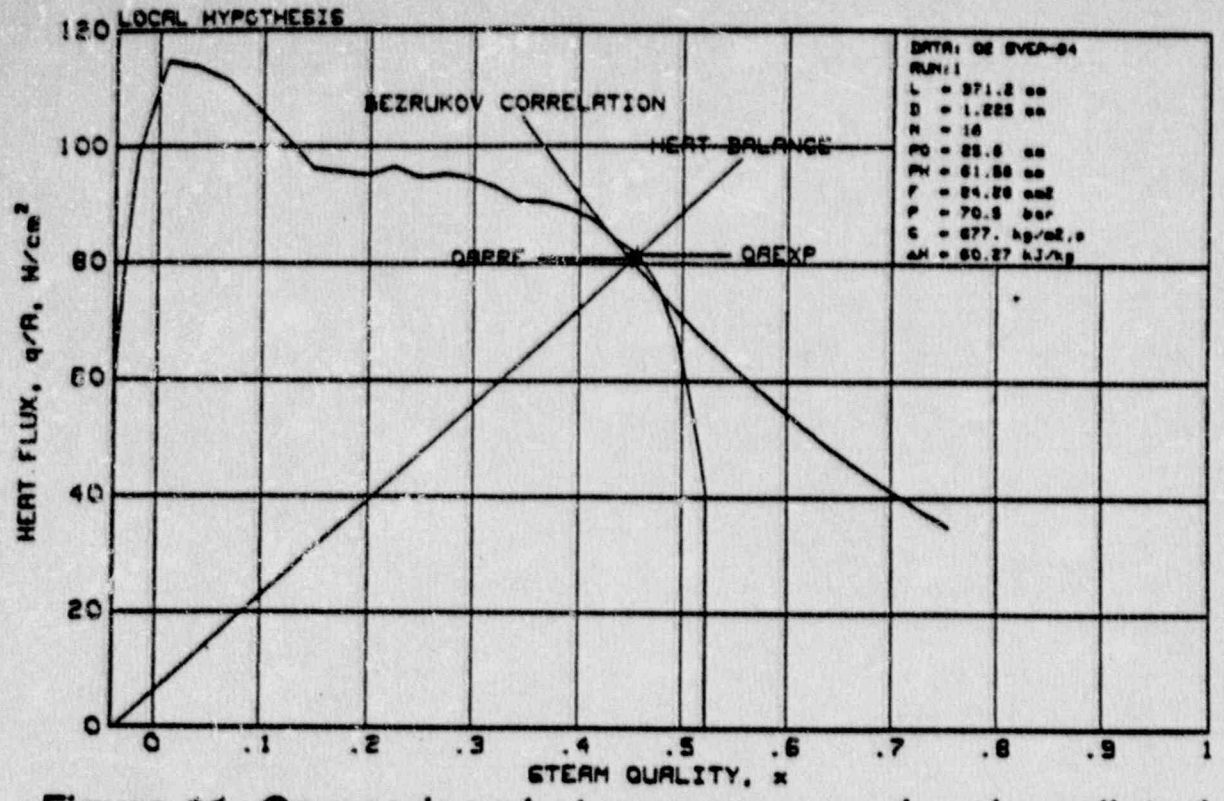

Figure 11. Comparison between measured and predicted dryout conditions. Bezrukov correlation

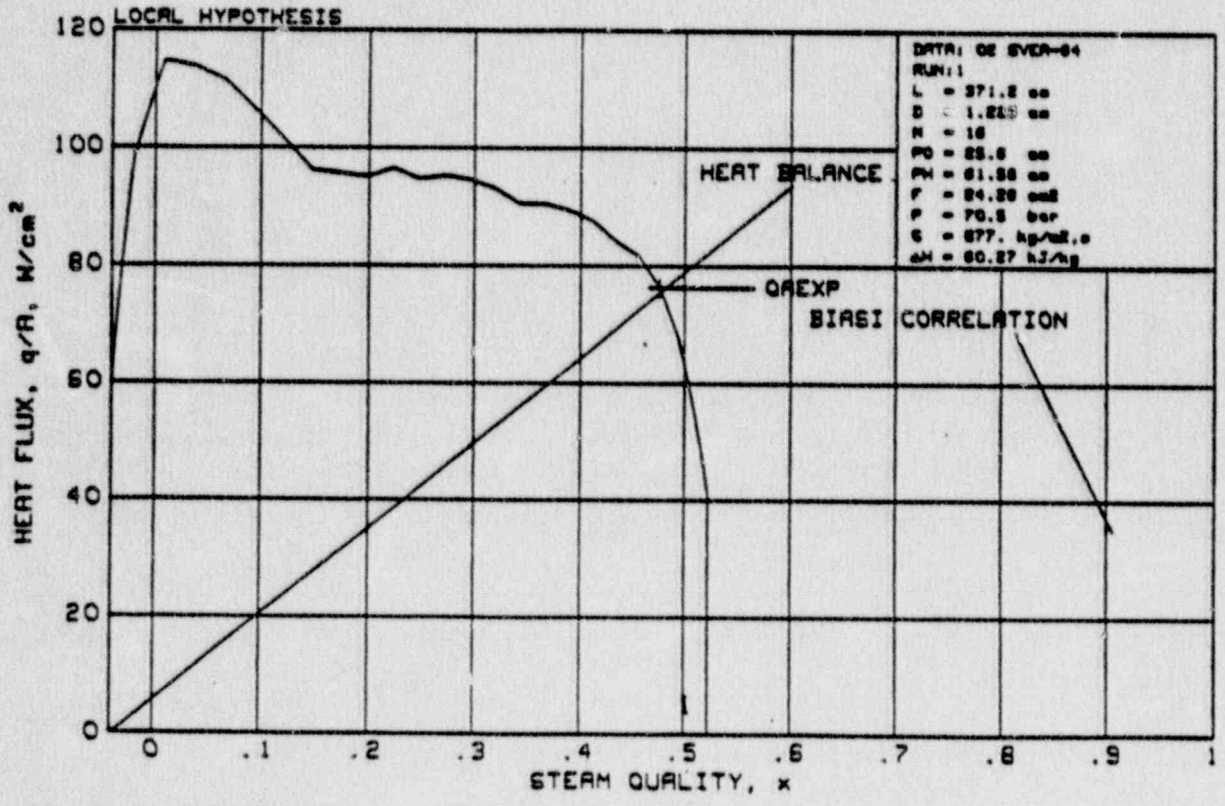

Figure 12.Comparison between measured and predicted dryout conditions.Biasi correlation

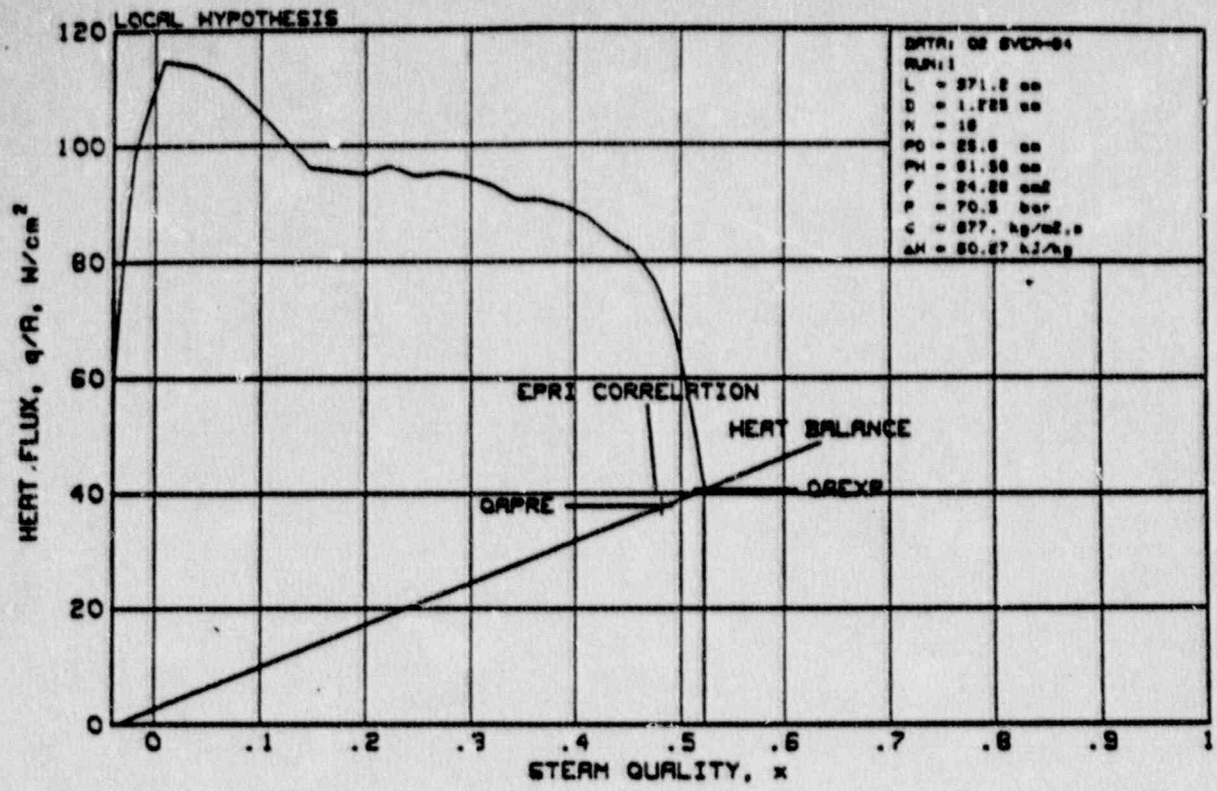

Figure 15.Comparison between measured and predicted dryout conditions.EPRI correlation

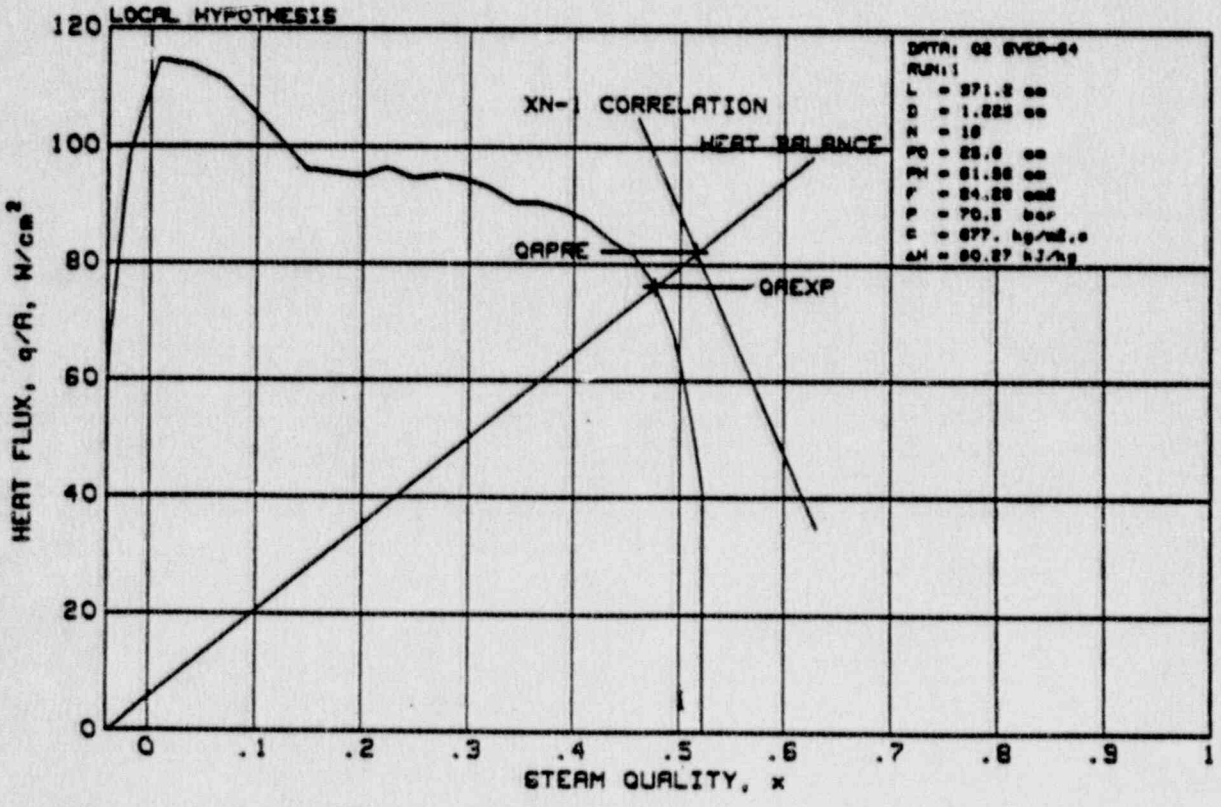

Figure 16.Comparison between measured and predicted dryout conditions.XN-1 correlation